

Yu C. Chang · Huan J. Keh

Creeping-flow rotation of a slip spheroid about its axis of revolution

Received: 25 April 2010 / Accepted: 12 August 2010 / Published online: 30 October 2010
© Springer-Verlag 2010

Abstract The problem of rotation of a rigid spheroidal particle about its axis of revolution in a viscous fluid is studied analytically and numerically in the steady limit of negligible Reynolds number. The fluid is allowed to slip at the surface of the particle. The general solution for the fluid velocity in prolate and oblate spheroidal coordinates can be expressed in an infinite-series form of separation of variables. The slip boundary condition on the surface of the rotating particle is applied to this general solution to determine the unknown coefficients of the leading orders, which can be numerical results obtained from a boundary collocation method or explicit formulas derived analytically. The torque exerted on the spheroidal particle by the fluid is evaluated for various values of the slip parameter and aspect ratio of the particle. The agreement between our hydrodynamic torque results and the available analytical solutions in the limiting cases is good. It is found that the torque exerted on the rotating spheroid normalized by that on a sphere with radius equal to the equatorial radius of the spheroid increases monotonically with an increase in the axial-to-radial aspect ratio for a no-slip or finite-slip spheroid and vanishes for a perfectly slip spheroid. For a spheroid with a specified aspect ratio, the torque is a monotonically decreasing function of the slip capability of the particle.

Keywords Particle rotation · Creeping flow · Prolate and oblate spheroids · Slip-flow surface · Hydrodynamic torque

1 Introduction

The translational and rotational motions of small particles in a continuous medium at low Reynolds numbers are of much fundamental and practical interest in the areas of chemical, biomedical, and environmental engineering and science. The theoretical treatment of this subject has grown out of the classic work of Stokes [1] for a rigid sphere moving in an unbounded viscous fluid. Oberbeck [2] and Jeffery [3] extended this result to the translation of an ellipsoid and rotation of a particle of revolution, respectively. More recently, the creeping flow caused by the motion of a particle of more general shape has been treated in the literature by a symbolic operator method [4], a boundary collocation method [5,6], a singularity method [7,8], and a boundary integral method [9,10].

When one tries to solve the Stokes problems, it is usually assumed that no slippage arises at the solid–fluid interfaces. Actually, this is an idealization of the transport processes involved. The phenomena that the adjacent fluid can slip frictionally over a solid surface occur for cases such as the rarified gas flow around an aerosol particle [11–13], the water flow near a hydrophobic surface [14–16], the micropolar fluid flow past a rigid particle [17], and the viscous fluid flow over the surface of a porous medium [18–20] or a small particle of

Communicated by Hussaini.

Y. C. Chang · H. J. Keh (✉)
Department of Chemical Engineering, National Taiwan University, 10617 Taipei, Taiwan, Republic of China
E-mail: huan@ntu.edu.tw

molecular size [21]. Presumably, any such slipping would be proportional to the local shear stress of the fluid next to the solid surface [22–24], known as the Navier slip (see Eq. 7), at least as the velocity gradient is small. The constant of proportionality, β^{-1} , is termed the slip coefficient of the solid surface. The quantity η/β (where η is the fluid viscosity) is a slip length defined by Navier/Maxwell and extensively used in the literature. It can be pictured by noting that the fluid motion is the same as if the solid surface was displaced inward by a distance η/β with the velocity gradient extending uniformly right up to no-slip velocity at the surface.

Basset [25] has found that the hydrodynamic torque experienced by a rotating rigid sphere of radius b with a slip-flow boundary condition at its surface is

$$T = 8\pi\eta b^3\Omega \frac{\beta b}{\beta b + 3\eta}, \quad (1)$$

where Ω is the angular velocity of the particle. When $\eta/\beta b = 0$, there is no slip at the particle surface and Eq. 1 reduces to the well-known Stokes result. In the limiting case of $\eta/\beta b \rightarrow \infty$, there is a perfect slip at the particle surface and the torque vanishes. Recently, the low-Reynolds-number motion of a rigid sphere with inhomogeneous slip boundary conditions was also analyzed by a perturbation method [26,27].

The problem of rotation of nonspherical particles with frictionally slip surfaces is obviously a matter of analytical difficulty. The friction coefficients for the uniform rotation of a perfect-slip spheroid in a viscous fluid ($\eta/\beta b \rightarrow \infty$) were computed numerically by fitting the slip condition approximately with a general solution of the Stokes equations in the form of an infinite series of spheroidal harmonics [21]. It was found that there is no torque when the perfect-slip spheroid is rotated about its axis of revolution, because no fluid is displaced. Recently, the low-Reynolds-number rotation of a rigid particle, which departs but little in shape from a sphere with the slip boundary condition [28], was analyzed, and an explicit expression for the hydrodynamic torque exerted on a spheroid was obtained to the second order in the small parameter characterizing the deformation from the spherical shape [29,30]. In this article, a general solution in the form of an infinite-series expansion for the creeping flow in spheroidal coordinates is used to investigate the Stokes problem of a slip prolate or oblate spheroidal particle rotating steadily about its axis of revolution. The torque acting on the spheroid by the ambient fluid as a function of the slip parameter and aspect ratio of the spheroid can be expressed in an approximate but explicit form and calculated numerically using a boundary collocation method. Our torque results agree quite well with the available analytical solutions in the limiting cases.

2 Analysis

We consider the rotational motion of a spheroidal particle about its axis of revolution in an incompressible, Newtonian fluid at the steady state, as shown in Fig. 1. The angular velocity of the particle equals $\Omega \mathbf{e}_z$, where \mathbf{e}_z is the unit vector in the positive z -direction. The fluid may slip frictionally at the surface of the particle and is at rest at infinity. The right-handed circular cylindrical coordinates (ρ, ϕ, z) and bifocal coordinates (ξ, φ, ϕ) [31–33] are established such that the surface of the spheroid is represented by $\xi = \xi_0$ or

$$\frac{z^2}{a^2} + \frac{\rho^2}{b^2} = 1, \quad (2)$$

where a and b are the half-length along the axis of revolution and the equatorial radius, respectively, of the spheroid. Depending on the aspect ratio of the spheroid, its shape can range widely from a needle (with $a/b \rightarrow \infty$) to a sphere (with $a/b = 1$) and to a circular disk (with $a/b \rightarrow 0$).

The Reynolds number is assumed to be sufficiently small so that the inertial terms in the fluid momentum equation can be neglected, in comparison with the viscous terms. Therefore, the fluid flow is governed by the Stokes equations,

$$\eta \nabla^2 \mathbf{v} - \nabla p = \mathbf{0}, \quad (3a)$$

$$\nabla \cdot \mathbf{v} = 0, \quad (3b)$$

where \mathbf{v} is the fluid velocity field and p is the dynamic pressure distribution. Evidently, for the axisymmetric rotational Stokes flow considered here, the dynamic pressure keeps constant everywhere and the only nonzero velocity component is $v_\phi(\xi, \varphi)$ in the ϕ direction. Thus, Eq. 3 becomes

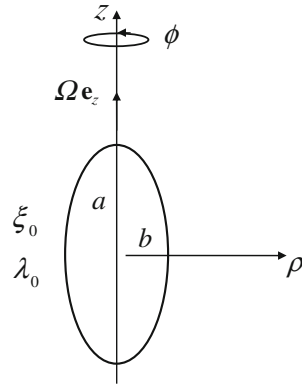


Fig. 1 Geometrical sketch for the rotation of a spheroidal particle about its axis of revolution

$$(\lambda^2 - 1) \frac{\partial^2 v_\phi}{\partial \lambda^2} + 2\lambda \frac{\partial v_\phi}{\partial \lambda} - \frac{v_\phi}{\lambda^2 - 1} + (1 - \omega^2) \frac{\partial^2 v_\phi}{\partial \omega^2} - 2\omega \frac{\partial v_\phi}{\partial \omega} - \frac{v_\phi}{1 - \omega^2} = 0, \quad (4)$$

where ω and λ are the variables related to the bifocal-coordinate transformations.

For prolate spheroids ($1 < a/b < \infty$), the coordinate transformation used is

$$\begin{aligned} \lambda &= \cosh \xi, & \omega &= \cos \varphi, \\ z &= c \cosh \xi \cos \varphi, & \rho &= c \sinh \xi \sin \varphi, \\ a &= c \cosh \xi_0, & b &= c \sinh \xi_0, \\ c &= (a^2 - b^2)^{1/2}, \end{aligned} \quad (5)$$

whereas for oblate spheroids ($0 < a/b < 1$), the coordinate transformation becomes

$$\begin{aligned} \lambda &= i \sinh \xi, & \omega &= \cos \varphi, \\ z &= ic \sinh \xi \cos \varphi, & \rho &= ic \cosh \xi \sin \varphi, \\ a &= ic \sinh \xi_0, & b &= ic \cosh \xi_0, \\ c &= -i(b^2 - a^2)^{1/2}. \end{aligned} \quad (6)$$

The origin (midpoint between the foci) of the bifocal coordinates (with $0 \leq \xi < \infty$ and $0 \leq \varphi \leq \pi$) has been set at the center of the spheroid, and the coordinate surface $\lambda = \lambda_0 = a/c$ corresponds to the surface of the spheroid defined by Eq. 2 or $\xi = \xi_0$. Note that the limiting case of $\xi_0 \rightarrow \infty$ or $\lambda_0 \rightarrow \infty$ represents a spheroid with $a/b = 1$ (a sphere).

The Navier slip condition states that the relative tangential velocity of the fluid at the particle surface is proportional to the local shear rate [22,26], and the fluid is motionless far away from the particle. Thus, the boundary conditions for the fluid velocity are

$$v_\phi = \rho \Omega + \frac{1}{\beta} \tau_{\lambda\phi} \quad \text{on } \lambda = \lambda_0, \quad (7)$$

$$v_\phi = 0 \quad \text{as } \lambda \rightarrow \infty, \quad (8)$$

where $1/\beta$ is the frictional slip coefficient about the particle surface, which is taken to be a constant, and $\tau_{\lambda\phi}$ is the fluid shear stress, which can be expressed in bifocal coordinates as

$$\tau_{\lambda\phi} = \eta \frac{\sqrt{\lambda^2 - 1}}{c \sqrt{\lambda^2 - \omega^2}} \left(\frac{\partial v_\phi}{\partial \lambda} - \frac{\lambda}{\lambda^2 - 1} v_\phi \right). \quad (9)$$

A general solution of Eq. 4 in bifocal coordinates can be obtained as a series expansion [3],

$$v_\phi = \Omega c \sum_{k=1}^{\infty} C_{2k-1} Q_{2k-1}^1(\lambda) P_{2k-1}^1(\omega), \quad (10)$$

where P_n^1 and Q_n^1 are the associated Legendre polynomials of the first and second kinds, respectively, of order n and degree 1, and C_n are unknown coefficients. Because v_ϕ is symmetric about the equatorial plane

$z = 0$, only the odd terms of the expansion in Eq. 10 are retained. Note that boundary condition Eq. 8 is immediately satisfied by a solution in the form of Eq. 10. For the particular case of a spheroid with a no-slip surface ($\eta/\beta b = 0$) rotating about its axis of revolution, only the first term of the infinite-series solution in Eq. 10 is needed for v_ϕ .

Applying Eq. 10 to boundary condition 7 at the particle surface, we obtain

$$\sum_{k=1}^{\infty} C_{2k-1} \left[Q_{2k-1}^1(\lambda_0) - \frac{\eta}{\beta c} g_{2k-1}(\lambda_0) \frac{\sqrt{\lambda_0^2 - 1}}{\sqrt{\lambda_0^2 - \omega^2}} \right] P_{2k-1}^1(\omega) = \sqrt{\lambda_0^2 - 1} \sqrt{1 - \omega^2}, \quad (11)$$

where

$$g_n(\lambda) = \frac{\partial Q_n^1(\lambda)}{\partial \lambda} - \frac{\lambda}{\lambda^2 - 1} Q_n^1(\lambda). \quad (12)$$

The unknown coefficients C_n in Eq. 10 are to be determined using Eq. 11.

The torque $T e_z$ acting on the particle by the fluid can be determined by the surface integral of the moment of stress about the axis of rotation [22], and the result is

$$T = -\frac{16}{3} \pi \eta c^3 \Omega C_1. \quad (13)$$

This expression shows that only the lowest-order coefficient C_1 contributes to the hydrodynamic torque experienced by the particle.

In the following two subsections, we present a boundary collocation method to obtain a numerical solution for the unknown coefficients C_n in Eq. 10 and an analytical method to result in explicit formulas for these coefficients of leading orders. The fluid velocity profile is completely obtained once these coefficients are solved.

2.1 Boundary collocation method

To satisfy the boundary condition 11 exactly along the entire semi-elliptic generating arc of the spheroid in a meridian plane would require the solution of the entire infinite array of the unknown constants C_n . However, the boundary collocation technique [34,35] enforces the condition at a finite number of discrete points on the particle's quarter-elliptic longitudinal arc (from $\varphi = 0$ to $\pi/2$, owing to the symmetry of the system geometry with respect to the plane $z = 0$) and truncates the infinite series in Eqs. 10 and 11 into finite ones. The unknown constants in the finite series permit one to satisfy the exact boundary condition at the discrete points on the particle surface. Thus, if the boundary is approximated by satisfying condition 11 at M discrete points, then the infinite series are truncated after M terms, resulting in a system of M simultaneous linear algebraic equations. This matrix equation can be solved by any of the standard matrix-reduction techniques to yield the M unknown constants C_n required in the truncated Eq. 10 for the fluid velocity. The accuracy of the truncation technique can be improved to any degree by taking a sufficiently large value of M . In principle, the truncation error vanishes as $M \rightarrow \infty$.

2.2 Analytical method

On the other hand, an analytical solution for the leading unknowns C_1, C_3, C_5 , etc. required in Eq. 10 for the fluid velocity can be found. To simplify the boundary condition given by Eq. 11, we multiply it by the function set $P_n^1(\omega)$, integrate with respect to ω from -1 to 1 , and utilize the orthogonality property of the associated Legendre polynomials in this interval to obtain

$$C_n s_{nn} Q_n^1(\lambda_0) - \frac{\eta}{\beta c} \sum_{k=1}^{\infty} C_{2k-1} x_{(2k-1)n} g_{2k-1}(\lambda_0) = \delta_{1n} s_{11} \sqrt{\lambda_0^2 - 1} \text{ for } n = 1, 3, 5, \dots, \quad (14)$$

where

$$s_{nn} = \int_{-1}^1 [P_n^1(\omega)]^2 d\omega, \quad (15a)$$

$$x_{jn} = \int_{-1}^1 \frac{\sqrt{\lambda_0^2 - 1}}{\sqrt{\lambda_0^2 - \omega^2}} P_j^1(\omega) P_n^1(\omega) d\omega, \quad (15b)$$

and the dependence on ω disappears. In Eq. 14, δ_{1n} is the Kronecker delta, which equals unity if $n = 1$ and vanishes otherwise.

If Eq. 10 for the fluid velocity is truncated after N terms, the first N equations of Eq. 14 can be used to solve the N unknown constants C_n . Similar to the case in the previous subsection, the accuracy will be acceptable when the value of N is sufficiently large. Again, the truncation error disappears as $N \rightarrow \infty$. In the Appendix, the two algebraic equations required to solve the unknown coefficients C_1 and C_3 and their explicit solution are given for a specific case that Eq. 10 is truncated after two terms ($N = 2$). Although we have also obtained the explicit solution for the unknown coefficients C_1 , C_3 , and C_5 for the more accurate case of $N = 3$, its formulas are not presented here for conciseness.

3 Results and discussion

For a spheroidal particle with a no-slip surface ($\eta/\beta b = 0$) rotating with an angular velocity Ω about its axis of revolution in an unbounded fluid, the exact solution for the torque exerted on the particle by the fluid is [3]

$$T_\infty = 8\pi\eta b^3 \Omega \left\{ \frac{3}{2} (\lambda_0^2 - 1)^{1/2} [\lambda_0 - (\lambda_0^2 - 1) \coth^{-1} \lambda_0] \right\}^{-1}. \quad (16)$$

In this section, we first present the numerical results of the hydrodynamic torque experienced by a slip spheroidal particle undergoing steady rotation about its axis of revolution obtained by using the boundary collocation method described in Sect. 2.1. Then, the leading-order asymptotic solutions for this torque resulting from the analytical method introduced in Sect. 2.2 will be given and compared with the convergent collocation solutions.

3.1 Boundary collocation solutions

The system of linear algebraic equations to be solved for the coefficients C_n using the boundary collocation method is constructed from Eq. 11. When specifying the M points along the quarter-elliptic generating arc of the spheroid where the boundary condition 7 or 11 is to be exactly satisfied, the first point that should be chosen is $\varphi = \pi/2$ (or $\omega = 0$), since this point defines the projected area of the particle normal to its axis of revolution. In addition, the point $\varphi = 0$ (or $\omega = 1$) is also important. However, an examination of the system of linear algebraic equations in the truncated form of Eq. 11 shows that the matrix equation becomes singular if these points are used. To overcome this difficulty, these points are replaced by closely adjacent points, i.e., $\varphi = \delta$ and $\pi/2 - \delta$ [8, 24, 34]. Additional points along the boundary are selected to divide the quarter-elliptic arc of the spheroid into segments with equal angles in φ . The range of optimum values of δ has been found to be quite broad, and here we use 0.01° , with which the numerical results of the hydrodynamic torque acting on the particle converge satisfactorily. In principle, as long as the number of the collocation points is sufficiently large and the distribution of the collocation points is adequate, the solution of the torque will converge and the shape of the particle can be well approximated.

Hydrodynamic torques about the axis of revolution, calculated using the boundary collocation method, are presented in Tables 1 and 2 for a prolate spheroid and an oblate spheroid, respectively. Values are normalized by the torque on a sphere with radius equal to the maximum cross-sectional radius of the spheroid ($8\pi\eta b^3 \Omega$). Several representative cases of the axial-to-radial aspect ratio a/b and the slip parameter $\eta/\beta b$ are presented. All of the results were obtained by increasing the number of collocation points M until the calculated value

Table 1 Leading-order asymptotic results (with $N = 2$ and $N = 3$) and boundary collocation results of the dimensionless torque for the rotation of a prolate spheroid about its axis of revolution for various values of the aspect ratio and slip parameter of the spheroid

$\eta/\beta b$	M or N	$T/8\pi\eta b^3\Omega$					
		$a/b = 1$	$a/b = 1.1$	$a/b = 2$	$a/b = 5$	$a/b = 10$	$a/b = 20$
0	$N = 2$	1.00000	1.06017	1.61335	3.53040	6.80471	13.4239
	$M = 4$	(1.00000)	(1.06017)	(1.61335)	(3.53040)	(6.80471)	(13.4239)
	Exact solution	1.00000	1.06017	1.61335	3.53040	6.80471	13.4239
0.1	$N = 2$	0.76923	0.81903	1.27410	2.83840	5.50004	10.8726
	$N = 3$	0.76923	0.81903	1.27414	2.83896	5.50151	10.8757
	$M = 14$	(0.76923)	(0.81903)	(1.27414)	(2.83908)	(5.50201)	(10.8770)
	Approximate solution	0.76923	0.81903	1.27569	2.90804	6.00525	13.6120
1	$N = 2$	0.25000	0.26883	0.44258	1.03872	2.04511	4.06769
	$N = 3$	0.25000	0.26883	0.44262	1.03931	2.04685	4.07161
	$M = 10$	(0.25000)	(0.26883)	(0.44262)	(1.03937)	(2.04709)	(4.07223)
	Approximate solution	0.25000	0.26883	0.44598	1.13571	2.62455	6.87455
3	$N = 2$	0.10000	0.10784	0.18079	0.43226	0.85625	1.70711
	$N = 3$	0.10000	0.10784	0.18080	0.43248	0.85691	1.70861
	$M = 10$	(0.10000)	(0.10784)	(0.18080)	(0.43250)	(0.85699)	(1.70882)
	Approximate solution	0.10000	0.10785	0.18270	0.48715	1.18247	3.27767
10	$N = 2$	0.03226	0.03483	0.05889	0.14207	0.28228	0.56345
	$N = 3$	0.03226	0.03483	0.05889	0.14214	0.28247	0.56390
	$M = 8$	(0.03226)	(0.03483)	(0.05889)	(0.14215)	(0.28250)	(0.56396)
	Approximate solution	0.03226	0.03484	0.05959	0.16239	0.40305	1.14440

The values in parentheses are boundary collocation results; exact and approximate solutions are calculated using Eqs. 16 and 17, respectively

Table 2 Leading-order asymptotic results (with $N = 2$ and $N = 3$) and boundary collocation results of the dimensionless torque for the rotation of an oblate spheroid about its axis of revolution for various values of the aspect ratio and slip parameter of the spheroid

$\eta/\beta b$	M or N	$T/8\pi\eta b^3\Omega$				
		$a/b = 0.9$	$a/b = 0.5$	$a/b = 0.2$	$a/b = 0.1$	$a/b = 0.05$
0	$N = 2$	0.94018	0.70502	0.53437	0.47894	0.45156
	$M = 4$	(0.94018)	(0.70502)	(0.53437)	(0.47894)	(0.45156)
	Exact solution	0.94018	0.70502	0.53437	0.47894	0.45156
0.1	$N = 2$	0.71962	0.52327	0.37799	0.32878	0.30243
	$N = 3$	0.71962	0.52334	0.37966	0.33343	0.31065
	$M = 24$	(0.71962)	(0.52335)	(0.38009)	(0.33541)	(0.31517)
	Approximate solution	0.71962	0.52306	0.37762	0.32952	0.30554
1	$N = 2$	0.23134	0.15949	0.11185	0.09834	0.09197
	$N = 3$	0.23134	0.15953	0.11266	0.10034	0.09518
	$M = 22$	(0.23134)	(0.15953)	(0.11279)	(0.10089)	(0.09640)
	Approximate solution	0.23133	0.15837	0.10543	0.08812	0.07953
3	$N = 2$	0.09225	0.06277	0.04395	0.03890	0.03661
	$N = 3$	0.09225	0.06279	0.04425	0.03964	0.03781
	$M = 18$	(0.09225)	(0.06279)	(0.04430)	(0.03985)	(0.03828)
	Approximate solution	0.09225	0.06217	0.04061	0.03360	0.03014
10	$N = 2$	0.02972	0.02011	0.01407	0.01249	0.01179
	$N = 3$	0.02972	0.02011	0.01417	0.01273	0.01217
	$M = 18$	(0.02972)	(0.02011)	(0.01418)	(0.01279)	(0.01232)
	Approximate solution	0.02972	0.01989	0.01289	0.01062	0.00950

The values in parentheses are boundary collocation results; exact and approximate solutions are calculated using Eqs. 16 and 17, respectively

changed by less than 1×10^{-5} for addition of a single point. The exact solution of $T/8\pi\eta b^3\Omega$ for the axisymmetric rotation of a no-slip spheroid (with $\eta/\beta b = 0$) given by Eq. 16 is also given in these tables for comparison. It can be seen that our results from the boundary collocation method agree excellently with the exact solution in this limit. In general, the convergence behavior of the collocation method is very good, even for the relatively difficult case of large or small axial-to-radial aspect ratio a/b .

Our numerical results of the dimensionless torque $T/8\pi\eta b^3\Omega$ for the axisymmetric rotation of a prolate spheroid and an oblate spheroid as a function of the aspect ratio a/b for several different values of the slip parameter $\eta/\beta b$ are plotted in Figs. 2 and 3, respectively. As indicated in Eq. 1, this dimensionless torque

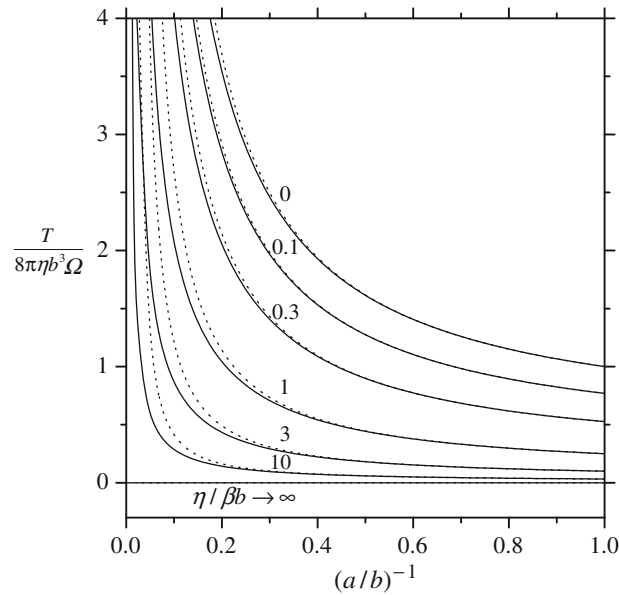


Fig. 2 Plots of the dimensionless torque for the rotation of a prolate spheroid with a slip surface about its axis of revolution versus the inverse aspect ratio $(a/b)^{-1}$ for various values of the slip parameter $\eta/\beta b$. The *solid* and *dotted* curves represent the boundary collocation solutions and approximate solutions given by Eq. (17), respectively

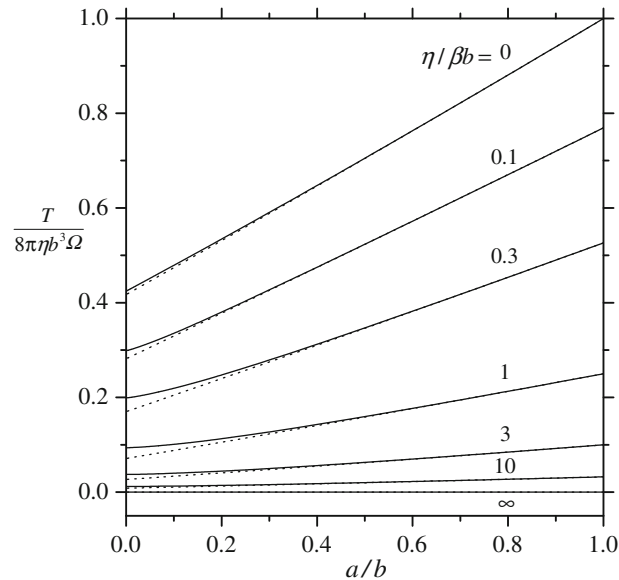


Fig. 3 Plots of the dimensionless torque for the rotation of an oblate spheroid with a slip surface about its axis of revolution versus the aspect ratio a/b for various values of the slip parameter $\eta/\beta b$. The *solid* and *dotted* curves represent the boundary collocation solutions and approximate solutions given by Eq. (17), respectively

equals $1/(1 + 3\eta/\beta b)$ for the special case of a slip sphere (with $a/b = 1$). For a prolate spheroid with a no-slip surface ($\eta/\beta b = 0$) or a slip surface having a finite value of $\eta/\beta b$, as shown in Fig. 2, the value of $T/8\pi\eta b^3\Omega$ increases monotonically with an increase in the value of a/b because of the increase in the surface area with an increase in a/b for a given value of the equatorial radius b . For a perfectly slip spheroid (with $\eta/\beta b \rightarrow \infty$), $T/8\pi\eta b^3\Omega$ disappears irrespective of its aspect ratio, consistent with the prediction from previous analyses [21,30]. On the other hand, $T/8\pi\eta b^3\Omega$ is a monotonically decreasing function of $\eta/\beta b$ for a given shape of spheroid, and its dependence becomes sensitive when the value of a/b is large (say, greater than 5). It can be seen that the hydrodynamic torque on the spheroid can be large when a/b is large and $\eta/\beta b$ is small.

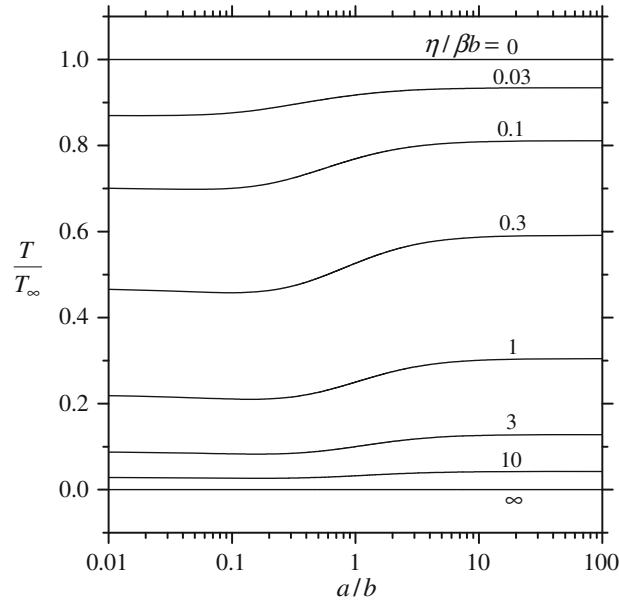


Fig. 4 Plots of the normalized torque T/T_∞ for the rotation of a spheroid with a slip surface about its axis of revolution versus the aspect ratio a/b for various values of the slip parameter $\eta/\beta b$

Similar to the axisymmetric rotation of a prolate spheroid, the value of $T/8\pi\eta b^3\Omega$ decreases monotonically (and almost linearly) with a decrease in a/b for an oblate spheroid with a no-slip surface or a slip surface having a finite value of $\eta/\beta b$, as illustrated in Fig. 3. Again, $T/8\pi\eta b^3\Omega$ is a monotonically decreasing function of $\eta/\beta b$ for spheroids with a fixed value of a/b and vanishes for a full-slip spheroid (with $\eta/\beta b \rightarrow \infty$).

Recently, Chang and Keh [30] investigated the problem of slow flow of a viscous fluid past a slip particle whose shape deviates slightly from that of a sphere. Their analytical result corresponding to the hydrodynamic torque exerted on a spheroid rotating about its axis of revolution, which is correct to the second order in the small parameter $\varepsilon = 1 - (a/b)$ characterizing the deformation, can be expressed as

$$\frac{T}{8\pi\eta b^3\Omega} = \gamma_3 - \varepsilon \frac{3\gamma_3^2}{5\gamma_4} + \varepsilon^2 \frac{3\gamma_3^3\gamma_5}{175} (1 + 3\nu + 36\nu^2 + 150\nu^3), \quad (17)$$

where $\gamma_j = \beta b / (\beta b + j\eta)$ and $\nu = \eta/\beta b$. The values of the dimensionless torque $T/8\pi\eta b^3\Omega$ calculated from the approximate formula Eq. 17 are also listed in Tables 1 and 2 and plotted in Figs. 2 and 3 for comparison. It is found that the solution correct to the second order in ε given by Eq. 17 agrees well with our collocation solutions for small magnitudes of ε . The errors are less than 1.2% for particles with $0.5 \leq a/b \leq 2$. However, the accuracy of this approximate solution begins to deteriorate, as expected, when the value of a/b deviates from this range, especially for the case of an intensely slip spheroid.

In Fig. 4, the boundary collocation results of T/T_∞ , the torque for the axisymmetric rotation of a slip spheroid normalized by that of the spheroid with identical geometry but no slip at surface given by Eq. 16 (a characteristic value that accounts for the particle geometry), are plotted as a function of the axial-to-radial aspect ratio a/b for various values of the slip parameter $\eta/\beta b$. As expected, T/T_∞ equals unity for a no-slip spheroid (with $\eta/\beta b = 0$) and vanishes for a full-slip spheroid (with $\eta/\beta b \rightarrow \infty$), regardless of the value of a/b . Again, this normalized torque is a monotonically decreasing function of $\eta/\beta b$ for a specified shape of spheroid. Interestingly, for a spheroid with a given finite value of the slip parameter $\eta/\beta b$, the value of T/T_∞ decreases first with an increase in the value of a/b from a constant value as $a/b \rightarrow 0$, reaches a minimum at some value of a/b , and then increases with a further increase in a/b to another greater constant value as $a/b \rightarrow \infty$.

3.2 Asymptotic analytical solutions

As discussed in Sect. 2.2, the coefficients C_1, C_3, C_5 , etc. in Eq. 10 for the Stokes flow induced by a spheroid rotating about its axis of revolution can be solved explicitly using Eq. 14 when the infinite series are truncated

into finite N terms. In Tables 1 and 2, we also present the asymptotic results (with $N = 2$ and $N = 3$, whereas some cases of $N > 3$ can also be obtained but only the case of $N = 2$ is formulated in the Appendix for conciseness) of the nondimensional torque $T/8\pi\eta b^3\Omega$ for the axisymmetric rotation of a prolate spheroid and an oblate spheroid, respectively, for various values of the aspect ratio a/b and the slip parameter $\eta/\beta b$. One can see that, in general, the larger the value of N is (say, $N = 3$, where the analytical solution agrees excellently with the boundary collocation solutions obtained in the previous subsection for cases of a moderate aspect ratio in the range $0.2 \leq a/b \leq 5$), the more accurate the results will be. When the aspect ratio a/b deviates much from unity, the agreement between the approximate values of the hydrodynamic torque with $N = 3$ and the convergent collocation results is not as good as the cases with a/b close to unity. For the limiting case of no-slip spheroids (with $\eta/\beta b = 0$), only the first term of the infinite series in Eq. 10 is nonzero, and the explicit expression for the torque derived from Eqs. 13 and 14 is exactly the same as that given by Eq. 16.

4 Concluding remarks

The boundary-collocation numerical solutions and asymptotic analytical solutions for the hydrodynamic torque acting on a slip spheroidal particle undergoing slow and steady rotation about its axis of revolution in a viscous fluid are obtained in this article. The general solution for the fluid velocity in spheroidal coordinates is expressed as an infinite-series expansion, in which the unknown coefficients can be determined analytically to their leading orders and numerically with excellent convergence. It has been found that, for various values of the slip parameter $\eta/\beta b$ and axial-to-radial aspect ratio a/b of the prolate or oblate spheroidal particle, the agreement between our results of the hydrodynamic torque and the available analytical solutions in the limiting cases is good. The normalized torque $T/8\pi\eta b^3\Omega$ acting on the rotating spheroid increases monotonically with an increase in the aspect ratio a/b for a no-slip or finite-slip spheroid and vanishes for a perfectly slip spheroid. For a spheroid with a fixed aspect ratio, its hydrodynamic torque is a monotonically decreasing function of the slip parameter $\eta/\beta b$ of the spheroid.

We presented in the previous section only the results for a resistance problem, defined as that in which the torque T exerted by the surrounding fluid on the rotating particle is determined for a specified angular velocity Ω . In a mobility problem, on the other hand, the external torque T applied on the particle is specified and the angular velocity Ω will be determined. For the creeping rotation of a spheroidal particle about its axis of revolution considered in this work, the normalized angular velocity $8\pi\eta b^3\Omega/T$ for a mobility problem equals the reciprocal of the normalized torque given by Tables 1 and 2 as well as Figs. 2 and 3 for its corresponding resistance problem.

Acknowledgments This research was supported by the National Science Council of the Republic of China.

Appendix: analytical solution for the coefficients in Eq. 10 truncated after two terms

When Eq. 10 for the fluid velocity is truncated after two terms ($N = 2$),

$$v_\phi = \Omega c [C_1 Q_1^1(\lambda) P_1^1(\omega) + C_3 Q_3^1(\lambda) P_3^1(\omega)], \quad (\text{A1})$$

the boundary condition Eq. 14 for $n = 1$ and 3 becomes

$$\frac{4}{3}C_1 Q_1^1(\lambda_0) - \frac{\eta}{\beta c} [C_1 x_{11} g_1(\lambda_0) + C_3 x_{31} g_3(\lambda_0)] = \frac{4}{3}\sqrt{\lambda_0^2 - 1}, \quad (\text{A2})$$

$$\frac{24}{7}C_3 Q_3^1(\lambda_0) - \frac{\eta}{\beta c} [C_1 x_{13} g_1(\lambda_0) + C_3 x_{33} g_3(\lambda_0)] = 0, \quad (\text{A3})$$

where $g_n(\lambda)$ is defined by Eq. 12,

$$x_{11} = \lambda_0^2 - 1 + (\lambda_0^2 - 2)y, \quad (\text{A4a})$$

$$x_{13} = x_{31} = \frac{3}{8} [(15\lambda_0^2 - 14)(\lambda_0^2 - 1) + (15\lambda_0^4 - 24\lambda_0^2 + 8)y], \quad (\text{A4b})$$

$$x_{33} = \frac{2}{32} [(375\lambda_0^4 - 380\lambda_0^2 + 44)(\lambda_0^2 - 1) + (375\lambda_0^6 - 630\lambda_0^4 + 264\lambda_0^2 - 48)y], \quad (\text{A4c})$$

and

$$y = \sqrt{\lambda_0^2 - 1} \tan^{-1} \left(\frac{\sqrt{\lambda_0^2 - 1}}{1 - \lambda_0^2} \right). \quad (\text{A5})$$

Equations A2 and A3 are used to determine the coefficients C_1 and C_3 , and their result in explicit forms is

$$C_1 = \sqrt{\lambda_0^2 - 1} \left[\frac{24}{7} Q_3^1(\lambda_0) - \frac{\eta}{\beta c} x_{33} g_3(\lambda_0) \right] \Gamma, \quad (\text{A6a})$$

$$C_3 = \frac{\eta}{\beta c} \sqrt{\lambda_0^2 - 1} x_{13} g_1(\lambda_0) \Gamma, \quad (\text{A6b})$$

where

$$\Gamma = \left\{ \frac{24}{7} Q_1^1(\lambda_0) Q_3^1(\lambda_0) - \frac{\eta}{\beta c} \left[\frac{18}{7} x_{11} g_1(\lambda_0) Q_3^1(\lambda_0) + x_{33} g_3(\lambda_0) Q_1^1(\lambda_0) \right] + \frac{3}{4} \left(\frac{\eta}{\beta c} \right)^2 (x_{11} x_{33} - x_{13} x_{31}) g_1(\lambda_0) g_3(\lambda_0) \right\}^{-1}. \quad (\text{A7})$$

An explicit expression for the hydrodynamic torque experienced by a spheroid rotating about its axis of revolution results from Eqs. 13 and A6a. After the substitution of Eq. A6a into Eq. 13 taking $\eta/\beta b \rightarrow 0$, we obtain the explicit formula for the torque exerted on a no-slip spheroid given by Eq. 16. Taking $\eta/\beta b \rightarrow \infty$, we know that the torque vanishes from Eqs. A6a and 13.

References

1. Stokes, G.G.: On the effect of the internal friction of fluid on pendulums. *Trans. Cambridge Phil. Soc.* **9**, 8–106 (1851)
2. Oberbeck, A.: Uber stationare flussigkeitsbewegungen mit berucksichtigung der inner reibung. *J. Reine Angew. Math.* **81**, 62–80 (1876)
3. Jeffery, G.B.: On the steady rotation of a solid of revolution in a viscous fluid. *Proc. London Math. Soc.* **14**, 327–338 (1915)
4. Brenner, H.: The Stokes resistance of an arbitrary particle—part V. Symbolic operator representation of intrinsic resistance. *Chem. Eng. Sci.* **21**, 97–109 (1966)
5. Gluckman, M.J., Weinbaum, S., Pfeffer, R.: Axisymmetric slow viscous flow past an arbitrary convex body of revolution. *J. Fluid Mech.* **55**, 677–709 (1972)
6. Hsu, R., Ganatos, P.: The motion of a rigid body in viscous fluid bounded by a plane wall. *J. Fluid Mech.* **207**, 29–72 (1989)
7. Chwang, A.T., Wu, T.Y.: Hydrodynamic of low-Reynolds-number flow, part 2. Singularity method for Stokes flows. *J. Fluid Mech.* **67**, 787–815 (1975)
8. Keh, H.J., Tseng, C.H.: Slow motion of an arbitrary axisymmetric body along its axis of revolution and normal to a plane surface. *Int. J. Multiph. Flow* **20**, 185–210 (1994)
9. Youngren, G.K., Acrivos, A.: Stokes flow past a particle of arbitrary shape: A numerical method of solution. *J. Fluid Mech.* **69**, 377–403 (1975)
10. Staben, M.E., Zinchenko, A.Z., Davis, R.H.: Motion of a particle between two parallel plane walls in low-Reynolds-number Poiseuille flow. *Phys. Fluids* **15**, 1711–1733 (2003)
11. Keh, H.J., Shiau, S.C.: Effects of inertia on the slow motion of aerosol particles. *Chem. Eng. Sci.* **42**, 1621–1644 (2000)
12. Sharipov, F.: Application of the Cercignani-Lampis scattering kernel to calculations of rarefied gas flows. II. Slip and jump coefficients. *Eur. J. Mech. B Fluids* **22**, 133–143 (2003)
13. Sharipov, F., Kalempa, D.: Velocity slip and temperature jump coefficients for gaseous mixtures. I. Viscous slip coefficient. *Phys. Fluids* **15**, 1800–1806 (2003)
14. Trettheway, D.C., Meinhart, C.D.: Apparent fluid slip at hydrophobic microchannel walls. *Phys. Fluids* **14**, L9–L12 (2002)
15. Neto, C., Evans, D.R., Bonaccorso, E., Butt, H.J., Craig, V.S.J.: Boundary slip in Newtonian liquids: A review of experimental studies. *Rep. Prog. Phys.* **68**, 2859–2897 (2005)
16. Cottin-Bizonne, C., Steinberger, A., Cross, B., Raccart, O., Charlaix, E.: Nanohydrodynamics: The intrinsic flow boundary condition on smooth surfaces. *Langmuir* **24**, 1165–1172 (2008)
17. Sherif, H.H., Faltas, M.S., Saad, E.I.: Slip at the surface of a sphere translating perpendicular to a plane wall in micropolar fluid. *Z. Angew. Math. Phys.* **59**, 293–312 (2008)
18. Saffman, P.G.: On the boundary condition at the surface of a porous medium. *Stud. Appl. Math.* **50**, 93–101 (1971)
19. Nir, A.: Linear shear flow past a porous particle. *Appl. Sci. Res.* **32**, 313–325 (1976)
20. Keh, M.P., Keh, H.J.: Slow motion of an assemblage of porous spherical shells relative to a fluid. *Trans. Porous Med.* **81**, 261–275 (2010)
21. Hu, C.M., Zwanzig, R.: Rotational friction coefficients for spheroids with the slipping boundary condition. *J. Chem. Phys.* **60**, 4354–4357 (1974)

22. Happel, J., Brenner, H.: *Low Reynolds Number Hydrodynamics*. Nijhoff, The Netherlands (1983)
23. Keh, H.J., Chen, S.H.: The motion of a slip spherical particle in an arbitrary Stokes flow. *Eur. J. Mech. B Fluids* **15**, 791–807 (1996)
24. Keh, H.J., Huang, C.H.: Slow motion of axisymmetric slip particles along their axes of revolution. *Int. J. Eng. Sci.* **42**, 1621–1644 (2004)
25. Basset, A.B.: *A Treatise on Hydrodynamics*, vol 2. Dover, New York (1961)
26. Willmott, G.: Dynamics of a sphere with inhomogeneous slip boundary conditions in Stokes flow. *Phys. Rev. E* **77**, 055302-1-4 (2008)
27. Willmott, G.R.: Slip-induced dynamics of patterned and Janus-like spheres in laminar flows. *Phys. Rev. E* **79**, 066309-1-6 (2009)
28. Ramkissoon, H.: Slip flow past an approximate spheroid. *Acta Mech.* **123**, 227–233 (1997)
29. Senchenko, S., Keh, H.J.: Slipping Stokes flow around a slightly deformed sphere. *Phys. Fluids* **18**, 088104-1-4 (2006)
30. Chang, Y.C., Keh, H.J.: Translation and rotation of slightly deformed colloidal spheres experiencing slip. *J. Colloid Interface Sci.* **330**, 201–210 (2009)
31. Dassios, G., Hadjinicolaou, M., Payatakes, A.C.: Generalized eigenfunctions and complete semiseparable solutions for Stokes flow in spheroidal coordinates. *Quart. Appl. Math.* **52**, 157–191 (1994)
32. Deo, S., Datta, S.: Slip flow past a prolate spheroid. *Indian J. Pure Appl. Math.* **33**, 903–909 (2002)
33. Keh, H.J., Chang, Y.C.: Slow motion of a slip spheroid along its axis of revolution. *Int. J. Multiph. Flow.* **34**, 713–722 (2008)
34. Gluckman, M.J., Pfeffer, R., Weinbaum, S.: A new technique for treating multi-particle slow viscous flow: Axisymmetric flow past spheres and spheroids. *J. Fluid Mech.* **50**, 705–740 (1971)
35. Keh, H.J., Lee, T.C.: Axisymmetric creeping motion of a slip spherical particle in a nonconcentric spherical cavity. *Theor. Comput. Fluid Dyn.* **24**, 497–510 (2010)